The Biological Memory Effect in Microbial Fuel Cell Biosensors

Jianwei Zhang, *Member, IEEE*, Hao Ren, Suren Jayasuriya, *Member, IEEE*, Xiao-Jun Tian, and Junseok Chae

***Abstract*—Microbial fuel cells (MFCs) are electrochemical fuel cells that directly convert the chemical energy of organic compounds in biomass into electrical energy. Due to their self-sustainability, direct current output, and fast response, MFC biosensors have the potential for long-term environmental monitoring applications. For the first time, we report a biological memory effect (BME) in MFC biosensors during repeated toxin injections. The toxin response of the biosensors generally weakens over repeated toxin stimuli injection at low concentrations. Experimental results demonstrate that the current drop of the second and third toxin injection is only 48.88% and 28.13%, respectively, of the first toxin injection on average. To investigate this BME, an ordinary differential equation (ODE) model is established. By fitting ODE model parameters to the experimental results, the model successfully simulates the experiments and the BME. This ODE model has good potential to compensate for the BME with its predictive ability, and it may potentially correct inaccuracies that accrue during long-term environmental monitoring for MFC biosensors. The current research paves the way for implementing MFC biosensors for long-term environmental toxic chemical detection.**

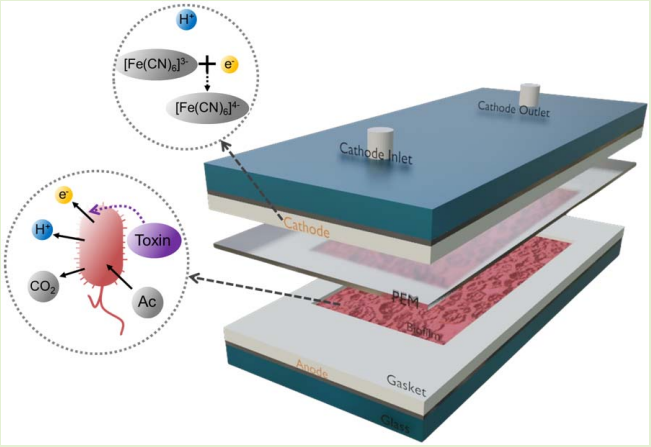

***Index Terms*— Biological memory effect (BME), biosensor, long-term monitoring, microbial fuel cell (MFC), toxin detection.**

I. Introduction

MICROBIAL fuel cells (MFCs) are bio-organic electrical devices composed of specific types of living bacteria, known as exoelectrogens or anode-respiring bacteria, which has the unique capability of transferring electrons generated during the metabolic process to outside its outer membrane [1]–[3]. Among all the microbes that can be implemented for MFC, *Geobacter sulfurrducens* is one of the most widely studied bacteria species due to its high current and power density. A typical two-chamber MFC is composed of one anode (anolyte filled) and one cathode (catholyte filled) chamber separated by a proton exchange membrane (PEM). The bacteria reproduces on the anode electrode and forms a biofilm, which decomposes organic material to generate electrons by the respiration process and transports the electrons to anode via extracellular electron transfer (EET) [4]. The power density of MFC can reach up to 7.72 W/m^2 and 11 220 W/m^3 [5], [6]. The MFCs have been widely studied in the fields of biomass to electricity conversion, waste water, and environmental treatment in the past two decades [7]–[11].

A main emerging application for MFCs is environmental long-term monitoring for the existence and concentration of toxic substances. Environmental monitoring is critical for the health of the environment, wildlife, and humans that may be exposed to these toxic substances [12], [13]. Although many other technologies have been reported to be ready for environmental monitoring [14]–[16], these methods cannot support long-term and consecutive monitoring due to the need to collect samples back to the lab or perform measuring on-site. Long-term toxic substance monitoring requires

Manuscript received 30 March 2022; revised 31 May 2022 and 9 July 2022; accepted 15 July 2022. Date of publication 3 August 2022; date of current version 14 September 2022. The associate editor coordinating the review of this article and approving it for publication was Dr. Levent Yobas. *(Jianwei Zhang and Hao Ren are co-first authors.) (Corresponding authors: Jianwei Zhang; Hao Ren.)*

Jianwei Zhang and Junseok Chae are with the School of Electrical, Computer and Energy Engineering, Arizona State University, Tempe, AZ 85281 USA (e-mail: jianwei.zhang@asu.edu).

Hao Ren is with the School of Information Science and Technology, Shanghai Tech University, Shanghai 201210, China, and also with the School of Electrical, Computer and Energy Engineering, Arizona State University, Tempe, AZ 85281 USA (e-mail: renhao@shanghaitech.edu.cn).

Suren Jayasuriya is with the School of Electrical, Computer and Energy Engineering and the School of Arts, Media and Engineering, Arizona State University, Tempe, AZ 85281 USA (e-mail: sjayasur@asu.edu).

Xiao-Jun Tian is with the School of Biological and Health Systems Engineering, Arizona State University, Tempe, AZ 85281 USA (e-mail: xiaojun.tian@asu.edu).

This article has supplementary downloadable material available at https://doi.org/10.1109/JSEN.2022.3194557, provided by the authors.

Digital Object Identifier 10.1109/JSEN.2022.3194557

self-powered, low-maintenance devices that can be easily deployed in the field.

MFCs have strong potential to serve as long-term toxic substance detection biosensors due to their advantage of self-powered, low maintenance, fast response [17], high sensitivity [18], and good self-sustainability [19]. They can be deployed in remote regions, and the sensor will power itself and collect data for a long time. By acquiring nutrients directly from the environment, such as from flowing creek, the MFC can be used as an energy source to drive low-power circuits for data sampling, storage, and transmission. Meanwhile, the fuel cell itself can also be used as an environmental sensor to detect the toxic substance. The MFC is highly sensitive for detecting low-concentration toxin [20], [21]. Recent studies have shown the feasibility of MFCs for detecting organic toxins and heavy metal ions for a short time [22], [23]. Pasternak *et al.* [24] implemented a self-powered MFC biosensor for online monitoring biological oxygen demand. Their MFC biosensor utilized the signal frequency to reflect the contaminant concentration and it continuously operated for 150 days.

In this article, we explore the feasibility of MFCs for long-term and low-concentration toxic substance monitoring. To the best of our knowledge, we conduct the first experiment where MFCs are exposed to repeated toxin injections at low concentrations. There are specific applications of interest such as fentanyl or other opioid drug detection that leverage toxins sensed in intervals. It is necessary for obtaining accurate toxin concentration estimation to study the effect of repeated low-concentration toxin injections on the MFC's response.

In particular, we observe a biological memory effect (BME) for MFCs with respect to repeated toxin injections. This BME is the phenomenon that the microbes progressively develop more significant resistance in facing repeated harmful stimuli. In essence, the more times the microbial community is exposed to an "unwanted" inhibitor, the more resistive they become, resulting in a decrease in the response amplitude. Other than evolution, changes in gene expression level and microbe community composition may also lead to this phenomenon as recent MFC studies have shown [25]–[27]. To date, no research on the BME or similar phenomenon in long-term monitoring of MFCs has been reported. Some researchers have injected a series of toxins. However, the toxin injection period or the toxin concentration was different when implementing experiments [19], [28].

In this article, we demonstrate the first experimental observation of a BME for MFCs where the electrical current response to repeated toxin injections weakens over time. To analyze the BME, we develop an ordinary differential equation (ODE) model with memory components to compensate for the BME by fitting with the experimental results. Our modeling method provides a solution for compensating the biosensor toxin response variation caused by the BME. The modeling method also provides a potential solution for adopting other living entities as environmental and toxin monitoring biosensor. This work provides a potential solution for the problem of BME to adopt the MFC as long-term biosensor in the future.

II. Experimental Procedure

A. Microscale MFC Biosensor Fabrication

In this study, we adopt our previously published microscale MFC structure for proceeding experiments. Two glass slides (microslides, $4.6 \times 2.6 \times 0.1$ cm^3, VWR) are used for electrode base of the anode and cathode. After drilling two through holes in the middle of glass slide for microfluidic inlet and outlet, Cr/Pt (20 nm/200 nm) films were deposited via sputtering (Emitech K675XD Turbo Sputter Coater). Then, the nanoports (10-32 coned, IDEX Health & Science) were aligned and glued to the two holes on the other side of glass slide. The microscale MFCs were assembled with a sandwich structure of electrodes, rubber gaskets, and PEM. The anode and cathode chambers are formed by carving a square pattern on the gaskets. The thickness of the gasket is 500 μm and the square pattern area is 100 mm^2, so the volume of two chambers both is 50 mm^3 (50 μL). The MFC biosensor structure diagram is shown in Fig. 1(a).

B. Inoculum, Anolyte, and Catholyte

The inoculum for the microscale MFC was obtained from an acetate-fed microbial electrolysis cell (MEC), which contained a Geobacter-enriched bacterial community originally from anaerobic-digestion sludge. *Geobacter sulfurreducens* accounts for 96%–98% of the microbial community. The anolyte was 25-mM sodium acetate medium with 1680-mg KH_2PO_4, 12 400-mg Na_2HPO_4, 1610-mg NaCl, 380-mg NH_4Cl, 5-mg EDTA, 30-mg $MgSO_4{\cdot}7H_2O$, 5-mg $MnSO_4{\cdot}H_2O$, 1-mg $Co(NO_3)_2$, 1-mg $CaCl_2$, 0.0001-mg $ZnSO_4{\cdot}7H_2O$, 0.1-mg $CuSO_4{\cdot}5H_2O$, 0.1-mg $AlK(SO_4)_2$, 0.1-mg H_3BO_3, 0.1-mg $Na_2MoO_4{\cdot}2H_2O$, 0.1-mg Na_2SeO_3, 0.1-mg $Na_2WO_4{\cdot}2H_2O$, 0.2-mg $NiCl_2{\cdot}6H_2O$, and 1-mg $FeSO_4{\cdot}7H_2O$ (per liter of distilled water) (pH 7.8 ± 0.2). The catholyte was composed of 100-mM potassium ferricyanide in a 100-mM phosphate buffer solution (pH 7.4).

In this study, formaldehyde is chosen as the toxic substance. The original formaldehyde solution was diluted by anolyte to get different concentrations (from 10^{-1} to 10^{-5} g/L) anolyte with toxin. The control anolyte (anolyte without toxin) was obtained by the same diluting procedure but replace the formaldehyde solution with distilled water.

C. Experiment Setup

For start-up, the inoculum was mixed with analyte by a Y-connector and injected into the microscale MFC anode chamber. Inoculum, anolyte, and catholyte were both injected by syringe pumps, and the injection flow rate was 120 μL/h. A 148-Ω resistor was implemented as load. The voltage drop of the load resistor was measured to obtain the output current of MFC. The start-up phase usually takes 3–9 days, as shown in Supplemental Figure S-A1. After MFC completes the start-up process, the inoculum was replaced with anolyte and the injection flow rate was kept at 120 μL/h. The MFC operation temperature was kept constant at 28 °C. The experiments were carried out after the MFC output current became stable (0.9 to 1.2 A/m^2). Fig. 1(b) shows the SEM photograph of Geobacter biofilm on the electrode.

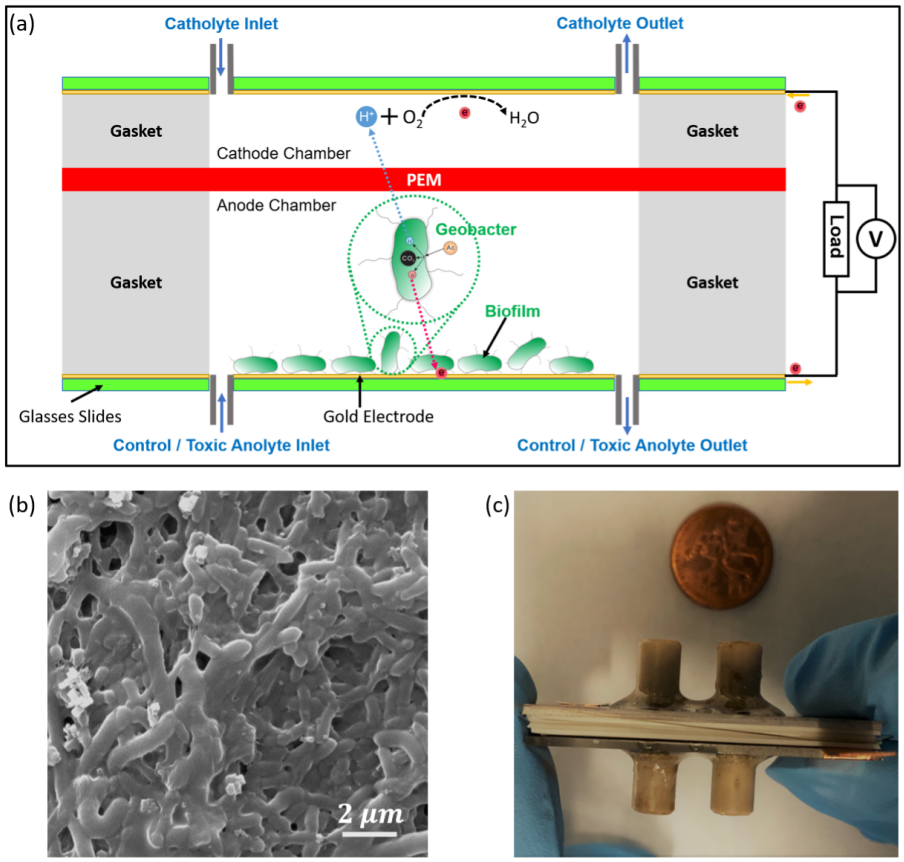

Fig. 1. (a) MFC biosensor structure diagram. Bacteria digests the acetate and generates carbon dioxide (CO_2), protons (H^+), and electrons (e^-). Electrons pass through outer load to the cathode electrode. The protons pass through the PEM to cathode and reduce at electrode with electrons and oxygen. The injected toxin will affect this process, which leads to the decrease of MFC output current. (b) SEM photograph of Geobacter biofilm on the anode electrode before exposure to formaldehyde. (c) Photograph of experiment MFC device.

The injection of toxic anolyte and control anolyte was controlled by syringe pumps with a Y-connector. When injecting the toxic anolyte, the toxic anolyte syringe pump continues to pump toxic anolyte into the MFC, while the control anolyte syringe pump stopped. In contrast, when injecting the control anolyte, the control anolyte syringe pump continues to pump, while the toxic anolyte syringe pump stopped. Before connecting the Y-connector to the device, the toxic anolyte and control anolyte were pumped continuously to make sure that there was no air inside the Y-connector.

In order to explore the BME, each experimental set included three consecutive toxic anolyte injection with the same toxin concentration (10^{-4} or 10^{-5} g/L) and injection period (1, 3, or 5 h), and the interval between injections start time was around 24 h. Although different concentrations of formaldehyde solution were prepared for experiment, only 10^{-4} or 10^{-5} g/L toxic anolyte was investigated. As shown in Supplemental Figure S-A2, a high concentration toxic anolyte of 0.1 g/L would kill the bacteria on the anode, and then, the MFC could not function after control anolyte injection.

For experimental data collection, a DAQ (National Instruments, USB-6216, sampling rate 10 Hz) was used to continuously record the MFC output current during the whole experimenting period (∼72 h). Before analyzing the data, a 0.5-Hz low-pass filter was applied to the collected data.

III. Results

Five experiments were conducted by following the methods described in Section II, and five original experimental results are provided in Supplemental Figures S-A3–S-A7, and the five experimental results are from five independent devices. To perform a system biology modeling analysis for the MFC biosensor in Section IV, the original results are normalized by following a standard procedure in system biology modeling [29], and certain regions, which contained measurement artifacts not related to the experiment, were removed. Fig. 2(a) and (b) shows two experimental normalized MFC biosensor current versus time results; the other three results are shown in Supplemental Figures S-A8–S-A10 for brevity. We have shown the raw data in the Supplemental Material, which provides more intuitive insights into experimental results.

For the first injection, the output current of the MFC displayed a characteristic dip due to the MFC's response to the toxic anolyte. This decrease occurs sometime after the anolyte is injected due to the MFC reaction time, typically on the order of 10 min. The output current decreases to a local minimum and then recovers back to the base current. Typical full-width at half-maximum (FWHM) measurements of the peaks were around 31% of the full width. Note that the rate of recovery is faster than the current decreasing. The shape of this

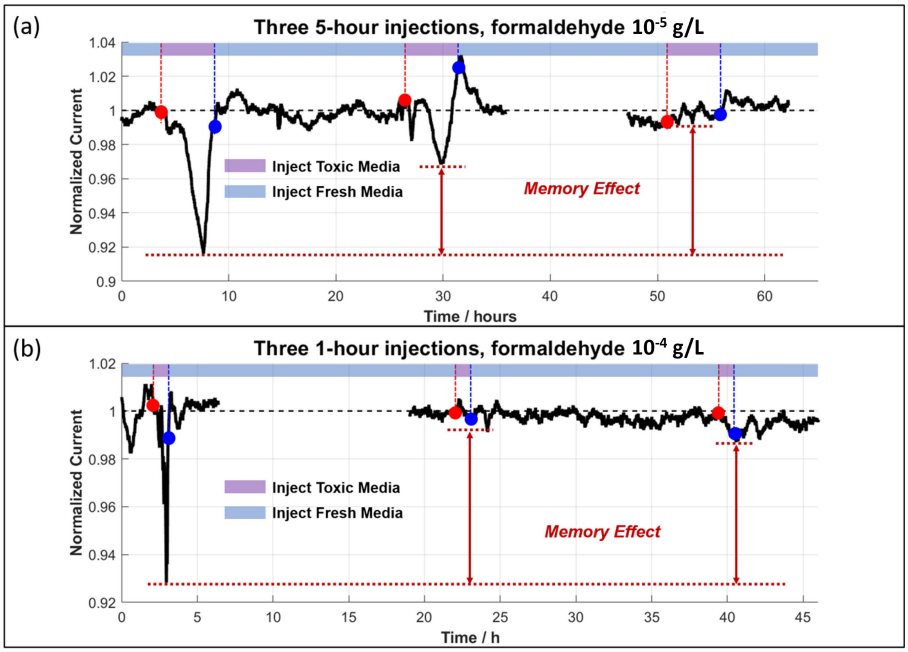

Fig. 2. BME existence in the MFC while performing toxin detection. Normalized experimental results, MFC biosensor output current versus time, for (a) three consecutive 5-h injections of 10^{-5} g/L toxic anolyte and (b) three consecutive 1-h injections of 10^{-4} g/L toxic anolyte. Red dots represent injecting toxic anolyte and blue dots represent injecting control anolyte. The MFC biosensor generated an obvious response to the first injection, but the responses to the second and third injections were much smaller or even not obvious.

MFC device response is in accordance with other experimental observations [17], [30], [31]. One key observation is that the current recovery actually starts, while the toxic anolyte is still being injected into the MFC. This phenomenon may be related to the low concentration of toxic anolyte being injected: the bacteria can potentially eliminate the toxin effects and recover. This also provides evidence why the BME occurs in the subsequent injections of the toxin.

Comparing the MFC response to the second and third toxin injections, all five experimental results display a BME, i.e., the MFC response weakens over each subsequent injection. Since the amount of current generated is approximately proportional to the number of active exoelectrogen, we calculate the relative drops in current compared to the base current to normalize across different experiments. We found that the average response due to the second injection was 44.8% of the first injection response, and the third response was 27.87% of the first injection response. In Table I, we present our analysis for these comparisons across the five experimental trials.

It is natural and inevitable for living entities to alter their activities and behaviors in response to environmental changes. For bacteria, the BME can happen at different levels, including genome, gene expression, and community structure. Bacteria genome change, caused by evolution, alters the whole community's behavior. For example, the bacteria can generate antibiotic resistance after long-term antibiotic treatment [32]. The BME can also be caused by bacteria gene expression levels increasing or decreasing. For example, Zhang *et al.* [25] found that the abundance of the silver resistance gene, *silE*, increases 50-fold after 41 days exposure to silver nanoparticles in the bacteria community. For the biosensor based on a mixed bacteria community, BME can also be produced by the shifting of dominant microbial species in the biofilm community [33], [34].

TABLE I
THREE DROP DEPTH COMPARISON RESULTS, ANALYZED IN PROPORTION OF BASE CURRENT, OF FIVE EXPERIMENTS AND THEIR FITTINGS

Experiment Trails	Exp/Fit Res	First	Second	Third
Figure 2 (a)	Exp	8.6%	5.6%	0.9%
	Fitting	8.21%	3.23%	0.82%
Figure 2 (b)	Exp	7.2%	1.0%	0.9%
	Fitting	7.15%	0.73%	1.04%
Figure S-A8	Exp	16.8%	14.6%	14.6%
	Fitting	17.31%	16.27%	14.41%
Figure S-A9	Exp	32.6%	24.0%	8.5%
	Fitting	31.03%	18.29%	8.93%
Figure S-A10	Exp	61.5%	3.0%	2.9%
	Fitting	60.34%	2.24%	5.21%

The main cause that induced BME in experiments is still unclear to us. Antimicrobial resistance development, gene expression-level change, and biofilm bacteria community composition change could all lead to this phenomenon. The bacteria community composition can change significantly within a short time after exposure to toxins [26]. In a previous study, it was reported that *Geobacter* showed strong resistance to formaldehyde [35]. It has been reported that some bacteria can develop antimicrobial resistance within two days [36], [37]. To clarify the real cause of BME, many future studies are needed, including biofilm community composition, gene mutations of bacteria, and RNA-seq data on relevant gene expression levels.

In addition, some other confounding factors cannot be ignored and need to be further explored with respect to

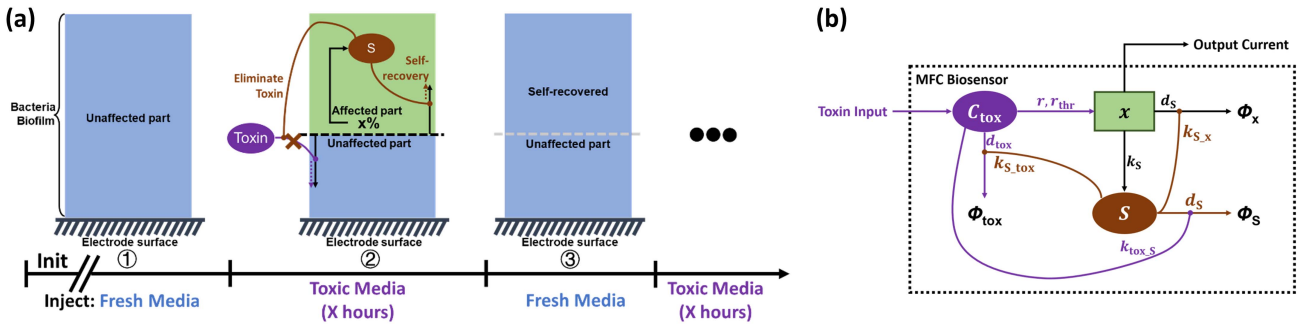

Fig. 3. (a) Theory diagram for ODE modeling. When the toxin reaches the anode chamber, the affected bacteria x will increase along with the toxin diffusion and perfusion. The affected bacteria generate certain antitoxin substances S to reduce the impacts from toxin and speed up bacteria self-recovery. (b) ODE model diagram based on theory diagram. Φ_S, Φ_{tox}, and Φ_x represent the decay of S, toxin, and x, respectively. S impacts toxin and x decay, and toxin impacts S decay. Toxin concentration C_{tox} impacts the x generation rate. S generation rate and MFC device output current are the determined by x value.

the BME observed experimentally. For example, although the five devices in this article are fabricated with the same procedure, the stabilized current and toxin response strength are inconsistent across the devices. A community phylogenetic analysis may help address this problem as in previous MFC studies [38], [39]. What is more, ferricyanide in the cathode introduces another variable to the whole system, which is associated with the respiration process of Geobacter. Previous studies by other researchers report that the reduction of ferricyanide to ferrocyanide shows a high reaction kinetics and supports a current density of more than 6 and 8 A/m^2 [40]–[42], suggesting that it may not be the bottleneck for the BME. However, because we have not measured the reaction kinetics of ferricyanide reduction to ferrocyanide in this study, the ferricyanide reduction rate and its impact on toxin resistance for MFC bacteria need to be further studied.

While the peak of the device response shows a BME, the duration of three responses has no clear trend with respect to BME. For example, a toxin injection with a period of 300 min corresponded to a response duration of 350 min for both the first and the second injection. In addition, the experiments all exhibited variation in the device responses due to nonexperimental factors. Each MFC device, while fabricated with the same process, has its own characteristic base current, bacteria population, pressure inside the chamber, and so on. This is why normalization is performed before experimental results are analyzed.

In summary, we demonstrate the existence of a BME across five experimental trials of our MFCs. Other studies [17], [19], [28] either perform one-time toxin injection to the system or increase the toxin concentration with subsequent injections as they study the sensor's response. In contrast, we keep the toxin concentration fixed to properly isolate the BME in our experiments. Our results suggest that the existence and influence of BME, which may be caused by gene expression-level changing and antimicrobial resistance developing jointly, should be carefully considered when utilizing MFCs for long-term toxin detection.

IV. Modeling the BME

In Section III, we conducted experiments that demonstrated the existence of a BME for MFC-based toxin biosensors. To gain better understanding of the dynamics of this process, we follow an approach inspired by systems biology [43] and control theory [44] via modeling the system as a set of ODEs.

A. Modeling

Based on the experimental results, the output current of MFC biosensors did not change much after exposure to the toxin, and we assume that the low concentration of toxin does not kill the bacteria and not change the composition of biofilm. The changes in total population and type composition of biofilm were not considered during modeling. Meanwhile, the external manifestation of bacterial antimicrobial resistance developing can also be interpreted as the changing gene expression levels, i.e., the appearance and expression of resistant gene mutations to toxins. Therefore, we consider the gene expression-level changing and antimicrobial resistance developing jointly as one parameter, the resistance to toxins. To model the BME, we determine the rate of toxin concentration change, affected bacteria ratio, and resistance to the toxin. The key variables related within the structure of the MFC are shown in Fig. 3(a). The *Geobacter sulfurreducens* forms a biofilm on the electrode surface after the MFC start-up process. When the toxin reaches the anode chamber, it affects the top part of the bacteria film, and the affected part x will increase along with the toxin diffusion and perfusion. The affected bacteria metabolism is inhibited by the toxin, and thus, the bacteria cannot efficiently generate electrons, which leads to a decrease in sensor output current. However, as shown experimentally, the affected bacteria over time develop a resistance to the toxin's impacts. To model this process, we assume that the affected bacteria generate certain antitoxin substances (noted as S) to eliminate the toxin by forming compounds with the toxin so that the toxin can no longer affect the bacteria and speed up bacteria self-recovery by promoting the expression of certain genes to rapidly recover the damaged organelles or proteins. It should be noted that substance S is merely hypothesized to explain the toxin resistance, and further study is needed to determine the precise biochemical process that underlies this phenomenon.

A set of ODE equations (1)–(3) is implemented to describe the relationship between three main variables: anode chamber

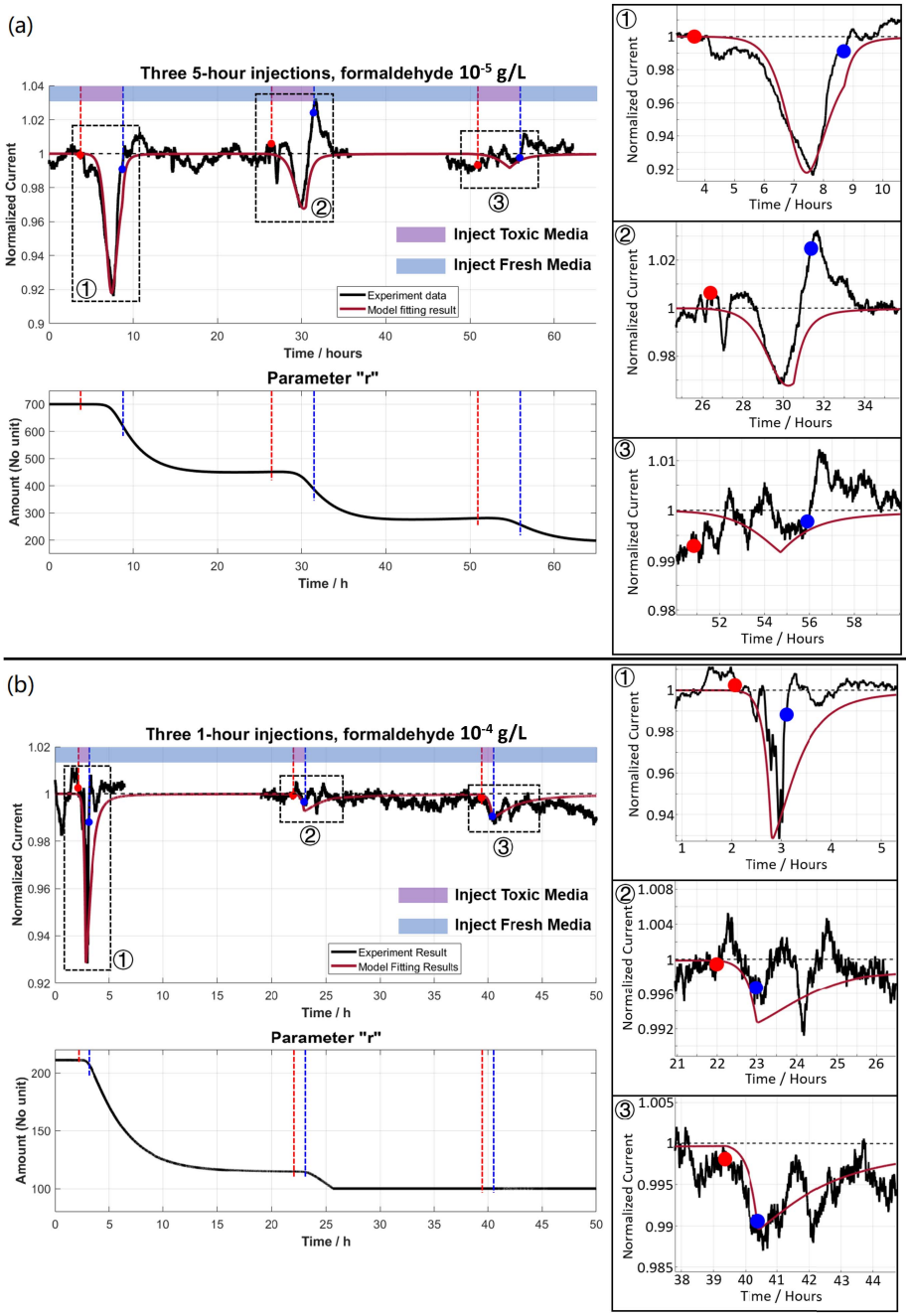

Fig. 4. Model fitting results of (a) three consecutive 5-h injections of 10^{-5} g/L toxic anolyte and (b) three consecutive 1-h injections of 10^{-4} g/L toxic anolyte. Red dots represent injecting toxic anolyte and blue dots represent injecting control anolyte. The fitting results show that the model can fit the experimental results well and have the potential to compensate for the BME.

toxin concentration C_{tox}, the affected bacteria x, and the antitoxin substance S. Their relationship is diagramed in Fig. 3(b)

$$\frac{d(C_{\text{tox}})}{dt} = \text{tox}_{\text{input}} - (d_{\text{tox}} + k_{\text{S\_tox}} \cdot S) \cdot C_{\text{tox}} \tag{1}$$

$$\frac{d(x)}{dt} = \frac{1}{1 + \exp(-r \cdot C_{\text{tox}} + r_{\text{thr}})} - (d_x + k_{S\_x} \cdot S) \cdot x \tag{2}$$

$$\frac{d(S)}{dt} = \frac{k_S \cdot x}{S + k_{S_{\text{shift}}}} - (d_S + k_{\text{tox\_S}} \cdot C_{\text{tox}}) \cdot S. \tag{3}$$

$\text{tox}_{\text{input}}$ represents the toxin input to the sensor, d_{tox} is the toxin self-decay rate, $k_{\text{S\_tox}}$ is the parameter describing the impacts of S on toxin decay rate, d_x is the self-recovery rate of the bacteria, k_{S_x} represents the impact of S on bacteria recovery, d_S is the self-decay rate of S, and $k_{\text{tox\_S}}$ is the C_{tox} impact on S's decay rate. $(k_s \cdot x/S + k_{S_{\text{shift}}})$ in (3) encodes the growth relationship of S affected by the bacteria x with rate k_S and $k_{S_{\text{shift}}}$ is a free parameter for model fitting.

Moffett *et al.* [45] observed that dose–response relationships in biology are typically modeled by a sigmoid function. We follow this approach by modeling $(1/1 + \exp(-r \cdot C_{\text{tox}} + r_{\text{thr}}))$ as the relationship between x increasing and toxin

concentration. r represents the bacteria resistance to the toxin, as r is smaller, the toxin resistance becomes higher. r_{thr} is the bacteria response threshold to the toxin. This r is the BME parameter in our model, i.e., the variation of r leads to the presence and strength of the BME in the system.

Equation (4) is used for describing r's variation as a function of the substance S

$$\frac{dr}{dt} = \begin{cases} -k_{S\_r} \cdot S \cdot \dfrac{r_{\text{base}}}{r} + r_{\text{rec}} & , r > r_{\text{limit}} \\ r_{\text{rec}} & , \text{otherwise} \end{cases} \tag{4}$$

where r_{base} is the initial value of r, k_{S_r} is the impact of S on r, r_{limit} is the minimum value possible, and r_{rec} is the self-recovery rate of r. In this article, $r_{\text{rec}} = (r_{\text{base}} - r) \cdot 10^{-6}$ is used. A piecewise function is adopted to clamp r to a minimum so that r cannot be negative, which causes unrealistic model outputs and instability.

Finally, what we observe is the output sensor current of the MFC in our experiments. Ren *et al.* [46] proposed a model to describe the MFC output current relationship with biological and chemical parameters where output current has a linear relationship with bacteria amount. The same relationship is adopted using the following equation:

$$\text{Output current} = 1 - \alpha \cdot x \tag{5}$$

where α is a fitting parameter.

Our model can simulate the experiment results and reproduce the BME well. After simulation and preliminary testing, our ODE model was used to fit actual experimental results. Please check "Section B—ODE model simulation" in the Supplementary Material for model simulation details.

B. Fitting Results

As discussed in the simulation section, one advantage of our model is that we only need to fit three free parameters to real experimental data: α, r_{base}, and k_{S_r}. The ratio between the first and second toxin responses from the data is used to fit k_{S_r}. Then, r_{base} is tuned to match the response curve shape of the model to the true sensor response. k_{S_r} and r_{base} are alternatively tuned until qualitatively good results are obtained. Finally, α is chosen to obtain the best fit to the data. The fitting only depends on the first and second toxin response curves.

The model fitting results for two example experimental trials [data: Fig. 2(a) and (b)] are shown in Fig. 4. The other three fitting results are shown in the Supplemental Figures S-A11–S-A13. All the fitting parameters are given in Supplemental Table S-1. Similar to the analysis for the real data, we also present the comparative analysis of the model in Table I. Based on the comparison results, all fitting results are within 3% of experimental results.

It is observed that the model can fit the experimental data well, including the shape and depths of the toxin response curves. Furthermore, the fit parameters are determined only by the first and second peaks, while the third peak is purely predicted by the model. This shows the potential of the model as a predictor for the response of MFC-based biosensors for subsequent toxin injections. After calibration, our model has the potential to predict the expected output current drop for certain toxin concentrations detected by the MFC biosensor, which can get a more accurate toxin concentration result other than misjudging a high concentration toxin with small output current drop as a lower concentration toxin. Indeed, one way to verify the model is to determine the concentration of injected toxic anolyte, i.e., fitting the first two toxic injections and then predicting toxin concentration for the following injections.

V. Conclusion

For the first time, we report a BME in MFC biosensors with respect to repeated toxin injections at low concentrations. It is found that the first toxin stimuli injection generally leads to a significant current drop, while the second and third injections only showed 48.88% and 28.13% current drop of the first injection on average in our experiments, respectively. An ODE model for the BME is presented based on mechanistic and system biology principles. The model fit the experimental results well and has the potential to compensate for data from MFCs with the BME. Future avenues of research include more experiments investigating changes in the biofilm's bacteria community, biofilm SEM figures before and after exposure to toxin, gene mutations related to antimicrobial resistance, additional toxic substances and their detection with MFCs, and the relationship of microbial growth and metabolic activity with MFC detection. What is more, the model we built in this article is a simple ODE model and is a preliminary solution. This model has a lot of room for optimization and needs to be supported by more experimental data.

References

[1] K. Rabaey, G. Lissens, S. D. Siciliano, and W. Verstraete, "A microbial fuel cell capable of converting glucose to electricity at high rate and efficiency," *Biotechnol. Lett.*, vol. 25, no. 18, pp. 1531–1535, 2003.

[2] C. I. Torres, A. K. Marcus, H.-S. Lee, P. Parameswaran, R. Krajmalnik-Brown, and B. E. Rittmann, "A kinetic perspective on extracellular electron transfer by anode-respiring bacteria," *FEMS Microbiol. Rev.*, vol. 34, no. 1, pp. 3–17, 2010.

[3] B. E. Logan and K. Rabaey, "Conversion of wastes into bioelectricity and chemicals by using microbial electrochemical technologies," *Science*, vol. 337, no. 6095, pp. 686–690, Aug. 2012.

[4] H. Ren, H.-S. Lee, and J. Chae, "Miniaturizing microbial fuel cells for potential portable power sources: Promises and challenges," *Microfluidics Nanofluidics*, vol. 13, no. 3, pp. 353–381, 2012.

[5] H. Ren, S. Rangaswami, H.-S. Lee, and J. Chae, "Enhanced current and power density of micro-scale microbial fuel cells with ultramicroelectrode anodes," *J. Micromech. Microeng.*, vol. 26, no. 9, Sep. 2016, Art. no. 095016.

[6] H. Ren, H. Tian, C. L. Gardner, T.-L. Ren, and J. Chae, "A miniaturized microbial fuel cell with three-dimensional graphene macroporous scaffold anode demonstrating a record power density of over 10000 W m^{-3}," *Nanoscale*, vol. 8, no. 6, pp. 3539–3547, 2016.

[7] R. M. Allen and H. P. Bennetto, "Microbial fuel-cells," *Appl. Biochem. Biotechnol.*, vol. 39, no. 1, pp. 27–40, 1993.

[8] H. J. Kim, S. H. Moon, and H. K. Byung, "A microbial fuel cell type lactate biosensor using a metal-reducing bacterium, shewanella putrefaciens," *J. Microbiol. Biotechnol.*, vol. 9, no. 3, pp. 365–367, 1999.

[9] B. E. Logan, C. Murano, K. Scott, N. D. Gray, and I. M. Head, "Electricity generation from cysteine in a microbial fuel cell," *Water Res.*, vol. 39, no. 5, pp. 942–952, 2005.

[10] L. Liu and S. Choi, "Self-sustaining, solar-driven bioelectricity generation in micro-sized microbial fuel cell using co-culture of heterotrophic and photosynthetic bacteria," *J. Power Sources*, vol. 348, pp. 138–144, Apr. 2017.

[11] N. N. M. Daud, A. Ahmad, A. A. Yaqoob, and M. N. M. Ibrahim, "Application of rotten rice as a substrate for bacterial species to generate energy and the removal of toxic metals from wastewater through microbial fuel cells," *Environ. Sci. Pollut. Res.*, vol. 28, no. 44, pp. 62816–62827, Nov. 2021.

[12] L. G. Olias and M. Di Lorenzo, "Microbial fuel cells for in-field water quality monitoring," *RSC Adv.*, vol. 11, no. 27, pp. 16307–16317, 2021.

[13] A. Adekunle, A. G. Vidales, L. Woodward, and B. Tartakovsky, "Microbial fuel cell soft sensor for real-time toxicity detection and monitoring," *Environ. Sci. Pollut. Res.*, vol. 28, no. 10, pp. 12792–12802, Mar. 2021.

[14] S. S. Nadar, P. D. Patil, M. S. Tiwari, and D. J. Ahirrao, "Enzyme embedded microfluidic paper-based analytic device (μPAD): A comprehensive review," *Crit. Rev. Biotechnol.*, vol. 41, no. 7, pp. 1046–1080, Oct. 2021.

[15] X. Chen, M. Leishman, D. Bagnall, and N. Nasiri, "Nanostructured gas sensors: From air quality and environmental monitoring to healthcare and medical applications," *Nanomaterials*, vol. 11, no. 8, p. 1927, Jul. 2021.

[16] P. Gong *et al.*, "Optical fiber sensors for glucose concentration measurement: A review," *Opt. Laser Technol.*, vol. 139, Jul. 2021, Art. no. 106981.

[17] W. Yang, X. Wei, A. Fraiwan, C. G. Coogan, H. Lee, and S. Choi, "Fast and sensitive water quality assessment: A μL-scale microbial fuel cell-based biosensor integrated with an air-bubble trap and electrochemical sensing functionality," *Sens. Actuators B, Chem.*, vol. 226, pp. 191–195, Apr. 2016.

[18] W. Yang, X. Wei, and S. Choi, "A dual-channel, interference-free, bacteria-based biosensor for highly sensitive water quality monitoring," *IEEE Sensors J.*, vol. 16, no. 24, pp. 8672–8677, Dec. 2016.

[19] D. Yu, L. Bai, J. Zhai, Y. Wang, and S. Dong, "Toxicity detection in water containing heavy metal ions with a self-powered microbial fuel cell-based biosensor," *Talanta*, vol. 168, pp. 210–216, Jun. 2017.

[20] C. Liao *et al.*, "Optimal set of electrode potential enhances the toxicity response of biocathode to formaldehyde," *Sci. Total Environ.*, vol. 644, pp. 1485–1492, Dec. 2018.

[21] H. Lu, Y. Yu, Y. Zhou, and F. Xing, "A quantitative evaluation method for wastewater toxicity based on a microbial fuel cell," *Ecotoxicol. Environ. Saf.*, vol. 183, Nov. 2019, Art. no. 109589.

[22] A. A. Yaqoob, M. N. M. Ibrahim, A. S. Yaakop, and A. Ahmad, "Application of microbial fuel cells energized by oil palm trunk sap (OPTS) to remove the toxic metal from synthetic wastewater with generation of electricity," *Appl. Nanosci.*, vol. 11, no. 6, pp. 1949–1961, Jun. 2021.

[23] S. Naik and S. E. Jujjavarapu, "Self-powered and reusable microbial fuel cell biosensor for toxicity detection in heavy metal polluted water," *J. Environ. Chem. Eng.*, vol. 9, no. 4, Aug. 2021, Art. no. 105318.

[24] G. Pasternak, J. Greenman, and I. Ieropoulos, "Self-powered, autonomous biological oxygen demand biosensor for online water quality monitoring," *Sens. Actuators B, Chem.*, vol. 244, pp. 815–822, Jun. 2017.

[25] C. Zhang, Z. Liang, and Z. Hu, "Bacterial response to a continuous long-term exposure of silver nanoparticles at sub-ppm silver concentrations in a membrane bioreactor activated sludge system," *Water Res.*, vol. 50, pp. 350–358, Mar. 2014.

[26] O. Obata, J. Greenman, H. Kurt, K. Chandran, and I. Ieropoulos, "Resilience and limitations of MFC anodic community when exposed to antibacterial agents," *Bioelectrochemistry*, vol. 134, Aug. 2020, Art. no. 107500.

[27] M. Xu *et al.*, "The evaluation of long term performance of microbial fuel cell based Pb toxicity shock sensor," *Chemosphere*, vol. 270, May 2021, Art. no. 129455.

[28] L. Zeng *et al.*, "$FePO_4$ based single chamber air-cathode microbial fuel cell for online monitoring levofloxacin," *Biosensors Bioelectron.*, vol. 91, pp. 367–373, May 2017.

[29] A. Krebs, J. Nyffeler, J. Rahnenführer, and M. Leist, "Normalization of data for viability and relative cell function curves," *Alternatives Animal Experimentation, ALTEX*, vol. 35, no. 2, pp. 268–271, 2018.

[30] Y. Jiang, P. Liang, X. Huang, and Z. J. Ren, "A novel microbial fuel cell sensor with a gas diffusion biocathode sensing element for water and air quality monitoring," *Chemosphere*, vol. 203, pp. 21–25, Jul. 2018.

[31] D. Wang *et al.*, "Open external circuit for microbial fuel cell sensor to monitor the nitrate in aquatic environment," *Biosensors Bioelectron.*, vol. 111, pp. 97–101, Jul. 2018.

[32] E. Christaki, M. Marcou, and A. Tofarides, "Antimicrobial resistance in bacteria: Mechanisms, evolution, and persistence," *J. Mol. Evol.*, vol. 88, no. 1, pp. 26–40, Jan. 2020.

[33] Y. Yi, B. Xie, T. Zhao, Z. Li, D. Stom, and H. Liu, "Effect of external resistance on the sensitivity of microbial fuel cell biosensor for detection of different types of pollutants," *Bioelectrochemistry*, vol. 125, pp. 71–78, Feb. 2019.

[34] A. Adekunle, V. Raghavan, and B. Tartakovsky, "On-line monitoring of heavy metals-related toxicity with a microbial fuel cell biosensor," *Biosensors Bioelectron.*, vol. 132, pp. 382–390, May 2019.

[35] H. Lu, Y. Yu, H. Xi, C. Wang, and Y. Zhou, "Bacterial response to formaldehyde in an MFC toxicity sensor," *Enzyme Microbial Technol.*, vol. 140, Oct. 2020, Art. no. 109565.

[36] M. Baym *et al.*, "Spatiotemporal microbial evolution on antibiotic landscapes," *Science*, vol. 353, no. 6304, pp. 1147–1151, Sep. 2016.

[37] A. Ferreiro, N. Crook, A. J. Gasparrini, and G. Dantas, "Multiscale evolutionary dynamics of host-associated microbiomes," *Cell*, vol. 172, no. 6, pp. 1216–1227, Mar. 2018.

[38] J. You, X. A. Walter, J. Greenman, C. Melhuish, and I. Ieropoulos, "Stability and reliability of anodic biofilms under different feedstock conditions: Towards microbial fuel cell sensors," *Sens. Bio-Sensing Res.*, vol. 6, pp. 43–50, Dec. 2015.

[39] O. Obata, M. J. Salar-Garcia, J. Greenman, H. Kurt, K. Chandran, and I. Ieropoulos, "Development of efficient electroactive biofilm in urine-fed microbial fuel cell cascades for bioelectricity generation," *J. Environ. Manage.*, vol. 258, Mar. 2020, Art. no. 109992.

[40] S. Zhao *et al.*, "Three-dimensional graphene/Pt nanoparticle composites as freestanding anode for enhancing performance of microbial fuel cells," *Sci. Adv.*, vol. 1, no. 10, Nov. 2015.

[41] K. Lawson, R. Rossi, J. M. Regan, and B. E. Logan, "Impact of cathodic electron acceptor on microbial fuel cell internal resistance," *Bioresource Technol.*, vol. 316, Nov. 2020, Art. no. 123919.

[42] Y. Liu, S. Guo, J. Wang, and C. Li, "Fundamental development and research of cathodic compartment in microbial fuel cells: A review," *J. Environ. Chem. Eng.*, vol. 10, no. 3, Jun. 2022, Art. no. 107918.

[43] U. Alon, *An Introduction to Systems Biology: Design Principles of Biological Circuits*. Boca Raton, FL, USA: CRC Press, 2019.

[44] D. E. Kirk, *Optimal Control Theory: An Introduction*. Chelmsford, MA, USA: Courier Corporation, 2004.

[45] D. B. Moffett, M. M. Mumtaz, D. W. Sullivan, and B. A. Fowler, "General considerations of dose-effect and dose-response relationships," in *Handbook on the Toxicology of Metals*. Amsterdam, The Netherlands: Elsevier, 2015, pp. 197–212.

[46] H. Ren *et al.*, "Regulating the respiration of microbe: A bio-inspired high performance microbial supercapacitor with graphene based electrodes and its kinetic features," *Nano Energy*, vol. 15, pp. 697–708, Jul. 2015.